Journal of Solid State Chemistry **147,** 146–153 (1999)
Article ID jssc.1999.8205, available online at http://www.idealibrary.com on IDEAL®

Solventothermal Synthesis and Structure of Lamellar Alkali Metal Selenidostannates(IV) $A_4Sn_4Se_{10} \cdot xH_2O$ with 20- ($A = Cs$; $x = 3.2$) and 36-Membered Pores ($A = K$, Rb; $x = 4.5, 1.5$)

Anja Loose and William S. Sheldrick[1]

Lehrstuhl für Analytische Chemie, Ruhr-Universität Bochum, D-44780 Bochum, Germany
E-mail: shel@anachem.ruhr-uni-bochum.de

Received October 22, 1998; in revised form February 5, 1999; accepted February 8, 1999

DEDICATED TO PROFESSOR JEAN ROUXEL, IN MEMORIAM

Treatment of A_2CO_3 ($A = K$, Rb) with Sn and Se in an H_2O/CH_3OH mixture at 130°C affords reaction solutions from which respectively $K_4Sn_4Se_{10} \cdot 4.5H_2O$ (1) and $Rb_4Sn_4Se_{10} \cdot 1.5H_2O$ (2) can be isolated on cooling. 1 crystallizes in the rhombohedral space group $R\bar{3}$ with $a = b = 15.320(3)$ Å, $c = 21.019(7)$ Å, $Z = 6$, $V = 4272(2)$ Å^3, 2 in the same space group with $a = b = 15.539(2)$ Å, $c = 21.373(4)$ Å, $Z = 6$, $V = 4469.4(13)$ Å^3. These isotypic phases contain lamellar $^{2}_{\infty}[Sn_4Se_{10}^{4-}]$ polyanions in which $SnSe_4^{4-}$ and $[Sn_2Se_6]^{4-}$ molecular building units are corner-bridged into a 6^3 net with 36-membered cavities of 1.3×1.4 nm cross-section. $Cs_4Sn_4Se_{10} \cdot 3.2H_2O$ (3) can be prepared under similar mild solventothermal conditions. It crystallizes in the triclinic space group $P\bar{1}$ with $a = 7.235(1)$ Å, $b = 9.468(2)$ Å, $c = 11.235(2)$ Å, $\alpha = 68.77(3)°$, $\beta = 83.25(3)°$, $\gamma = 84.53(3)°$, $Z = 1$, $V = 711.2(2)$ Å^3. In contrast to the 2-dimensional anions of the same formula type in 1 and 2, the $^{2}_{\infty}[Sn_4Se_{10}^{4-}]$ polyanions of 3 consist of $^{1}_{\infty}[SnSe_3^{2-}]$ ribbons that are corner-bridged through ditetrahedral $[Sn_2Se_6]^{4-}$ units into sheets with smaller 20-membered pores. The role of starting pH, cation size and temperature on the construction of lamellar selenidostannates(IV) are discussed. © 1999 Academic Press

INTRODUCTION

The technological potential of porous 2- and 3-dimensional polymeric thio- and selenidometalates(IV) of the heavier group 14 elements Ge and Sn as zeotype materials appears to have been discussed in depth for the first time in an article by Bedard *et al.* in 1989 (1). Subsequent synthetic and structural studies (2) on chalcogenidostannates(IV) have demonstrated that the marked propensity of Sn(IV) to expand its coordination sphere from tetrahedral in solution species such as SnE_4^{4-} or $Sn_2E_6^{4-}$ (E = S, Se) to trigonal bipyramidal (E = S, Se) or even octahedral (E = S) in the solid state allows the assembly of lamellar and framework anionic networks not available for Ge(IV) with its maximum coordination number of 4 in this class of compounds. Employment of a range of alkylammonium cations to direct the construction of thiostannate(IV) sheets under mild hydrothermal conditions has underlined the decisive role of space-filling and charge-compensation effects during the required self-assembly process (2, 3). As the size of the counterion increases from that of $[Cs(H_2O)_2]^+$ in $Cs_4Sn_5S_{12} \cdot 2H_2O$ (4) over Me_4N^+ and Et_4N^+ in $(R_4N)_2Sn_3S_7 \cdot xH_2O$ [R = Me, $x = 1$ (5); R = Et, $x = 0$ (6)] to that of $n\mathrm{Pr}_4N^+$ or $n\mathrm{Bu}_4N^+$ in $(R_4N)_2Sn_4S_9$ (7, 8) so does the size of the pores in the anionic networks from 20 to 24 and finally 32 members. This change in porosity is accompanied by a continuous increase in the condensation grade c ($= y/z$; 0.417, 0.429, 0.444) and a concomitant reduction in the average coordination number of the tin atoms (5.33, 5.0, 4.75) in these thiostannates(IV) $A_mSn_yS_z$. All three members of the series $^{2}_{\infty}[Sn_5S_{12}^{4-}]$, $^{2}_{\infty}[Sn_3S_7^{2-}]$, and $^{2}_{\infty}[Sn_4S_9^{2-}]$ contain characteristic Sn_3S_4 "semi-cubes" in which the tin atoms of an $(SnS)_3$ six-membered ring are bridged by a fourth sulfur atom. These molecular building blocks are linked into 6^3 nets in the polyanions of the type $^{2}_{\infty}[Sn_3S_7^{2-}]$ through shared $(SnS)_2$ rings, in which the participating tin atoms exhibit a trigonal bipyramidal coordination geometry.

An analogous lamellar anionic netwok has also been established for the selenidostannates(IV) $Cs_2Sn_3Se_7$ (9), $(enH_2)Sn_3Se_7 \cdot 0.5en$, and $(Me_2NH_2)_2Sn_3Se_7$ (10). These compounds were all prepared under mild methanolothermal conditions, as were the discrete di- and tritetrahedral anions in $Rb_4Sn_2Se_6$ (11), $Cs_4Sn_2Se_6$ (12), and $K_4Sn_3Se_8$ (13), the sheet anion $^{2}_{\infty}[Sn_2Se_6]^{2-}$ of $Cs_2Sn_2Se_6$ (14), and the framework anion $^{3}_{\infty}[Sn_2Se_5^{2-}]$ of $Rb_2Sn_2Se_5$ (15). In contrast to many hydrothermally synthesized thiostannates(IV)

---

[1] To whom correspondence should be addressed.

0022-4596/99 $30.00

[e.g., $Cs_4Sn_5S_{12} \cdot 2H_2O$ (4), $(Me_4N)_2Sn_3S_7 \cdot H_2O$ (5), $Rb_2Sn_3S_7 \cdot 2H_2O$ (11)] none of these selenidostannates(IV) contains solvent molecules in its solid state structure. The incorporation of water molecules in the coordination sphere of the structure-directing alkali metal cations will alter the effective size and shape of these counterions and will, therefore, influence the self-assembly of the anionic network (3). This state of affairs prompted us to study the construction of polymeric selenidostannates(IV) in a water/methanol mixture under mild solventothermal conditions in the expectation that novel lamellar networks might be favoured in the presence of aquated alkali metal cations.

This hypothesis has recently been confirmed by our synthesis of the isotypic phases $A_2Sn_4Se_9 \cdot H_2O$ (A = Rb, Cs) by reaction of A_2CO_3 with Sn and Se in an H_2O/CH_3OH mixture at 115–130°C (14). Their ${}^2_\infty[Sn_4Se_9^{2-}]$ polyanions contain cyclic Sn_4Se_5 molecular building units that are connected through $(SnSe)_2$ rings into sheets, whose 16-membered cavities are composed of just half the number of atoms found in the larger pores of the ${}^2_\infty[Sn_4S_9^{2-}]$ networks in $(R_4N)_2Sn_4S_9$ ($R = n\mathrm{Pr}_4N^+$, $n\mathrm{Bu}_4N^+$) (7,8). The average coordination number of the tin atoms in $A_2Sn_4Se_9 \cdot H_2O$ is only 4.50 as opposed to 4.75 in $(R_4N)_2Sn_4S_9$. We now report the preparation of three novel lamellar alkali metal selenidostannates(IV), $A_4Sn_4Se_{10} \cdot xH_2O$ (A = K, Rb, Cs), under mild solventothermal conditions in an H_2O/CH_3OH mixture. The condensation grade c of 0.40 in these phases is lower than those in the range 0.417–0.444 previously established for 2-dimensional chalcogenidostannates(IV) with exclusively Sn–E–Sn bridging.

EXPERIMENTAL SECTION

Syntheses

$K_4Sn_4Se_{10} \cdot 4.5H_2O$ (1). A glass tube (~10-ml capacity) containing 0.150 g (1.08 mmol) of K_2CO_3, 0.174 g (1.47 mmol) of Sn, and 0.225 g (2.85 mmol) of Se in 0.9 ml of a 1 : 2 H_2O/CH_3OH mixture was sealed under vacuum and heated to 130°C at a rate of $2°C \cdot h^{-1}$. After 72h at this temperature, the glass tube was cooled to 20°C at $1°C \cdot h^{-1}$ to afford bunches of orange-red prisms that were separated manually and washed with methanol to afford **1** in 27% yield (based on Se).

$Rb_4Sn_4Se_{10} \cdot 1.5H_2O$ (2). A glass tube (~10-ml capacity) containing 0.245 g (1.06 mmol) of Rb_2CO_3, 0.174 g (1.47 mmol) of Sn, and 0.225 g (2.85 mmol) of Se in 0.9 ml of a 1 : 2 H_2O/CH_3OH mixture was sealed under vacuum and heated to 130°C at a rate of $2°C \cdot h^{-1}$. After 96h at this temperature, the glass tube was cooled to 20°C at $1°C \cdot h^{-1}$ to afford a few black crystals of $Rb_2Sn_4Se_9 \cdot H_2O$ (14) (yield ca. 5%). Leaving the orange-yellow mother liquor to stand at −8°C for 72h led to the crystallization of **2** as orange prisms in 35% yield (based on Se).

$Cs_4Sn_4Se_{10} \cdot 3.2H_2O$ (3). A combination of 0.305 g (0.94 mmol) of Cs_2CO_3, 0.149 g (1.25 mmol) of Sn, and 0.202 g (2.56 mmol) of Se was heated in a 1 : 2 H_2O/CH_3OH mixture in a sealed glass tube to 130°C at a rate of $2°C \cdot h^{-1}$. After tempering for 24 h at this temperature, the glass tube was cooled to 20°C at $1°C \cdot h^{-1}$ to afford bunches of dark-red needles of **3** (yield = 38%, based on Se) that were separated manually from yellow plates of $Cs_4Sn_2Se_6$ (yield = 35%) (12).

X-ray Structural Analysis

All compounds were examined by X-ray powder diffraction to establish phase purity. Semiquantitative microprobe analysis (EDX) gave compositions consistent with those established by X-ray analysis. Calculated and observed XRD patterns were found to match well. Crystal and refinement data are listed for **1–3** in Table 1. Unit cell constants were obtained from the least-squares fit to the settings for 25 reflections (25° ≤ 2θ ≤ 30°) centered on a Siemens P4 diffractometer. Intensity data were collected on this instrument

TABLE 1

Crystal and Refinement Data for $K_4Sn_4Se_{10} \cdot 4.5H_2O$ (1), $Rb_4Sn_4Se_{10} \cdot 1.5H_2O$ (2) and $Cs_4Sn_4Se_{10} \cdot 3.2H_2O$ (3)

Compound	1	2	3
Space group	$R\bar{3}$	$R\bar{3}$	$P\bar{1}$
a (Å)	15.320(3)	15.539(2)	7.235(1)
b (Å)	15.320(3)	15.539(2)	9.468(2)
c (Å)	21.019(7)	21.373(4)	11.235(2)
α (°)	90	90	68.77(3)
β (°)	90	90	83.25(3)
γ (°)	120	120	84.53(3)
V (Å^3)	4272(2)	4469.4(13)	711.2(2)
Z	6	6	1
M	1501.8	1633.3	1853.63
$F(000)$	3966	4218	792
D_{calc} (g·cm^{-3})	3.50	3.64	4.33
Radiation	Mo$K\alpha$	Mo$K\alpha$	Mo$K\alpha$
μ (mm^{-1})	16.84	22.02	21.31
Crystal size (mm)	0.44 × 0.32 × 0.24	0.32 × 0.32 × 0.28	0.36 × 0.20 × 0.18
Absorption corr.	ψ scan	ψ scan	ψ scan
Max./min. transm.	0.065/0.024	0.044/0.013	0.079/0.033
$2\theta_{max}$ (°)	50	50	55
hkl range	0/15, 0/15, −24/24	0/17, −18/0, 0/25	0/9, −12/12, −14/14
Independent refl.	1565	1559	3041
R_{int}	0.030	0.057	0.032
$I > 2\sigma(I)$	1234	839	2441
Goodness of fit S	1.060	0.795	1.040
$R\ [I > 2\sigma(I)]^a$	0.045	0.048	0.062
wR_2 [all data]^b	0.112	0.116	0.182

[a] $R = \sum(|F_o| - |F_c|)/\sum|F_o|$.

[b] $wR_2 = [\sum w(F_o^2 - F_c^2)/\sum w(F_o^2)^2]^{1/2}$ with weights given by $w = [\sigma^2(F_o^2) + (aP)^2 + bP)^{-1}$ with $P = [\max(F_o^2, 0) + 2F_c^2]/3$.

in the ω mode at 293 K. Significant deviations in intensity were not observed for three selected reflections that were monitored during the course of data collection for each of the compounds. Semiempirical absorption corrections were performed on the basis of ψ scans for nine chosen reflections with high χ values. After structure solution with SHELXS-86 (16), positional parameters and anisotropic temperature factors were refined against F_o^2 with SHELXL-93 (17). The alkali metal cations K1 and Rb1 in the isotypic phases **1** and **2** (Table 2) are positioned on a crystallographic C_3 axis, as are Sn1 and Se1 of the anionic network. O1 in the coordination sphere of K1/Rb1 is disordered in both structures on a general position with a partial occupation factor (SOF) of 0.5. The remaining two cation/solvent sites in the asymmetric units of these compounds are occupied by K2 and O2 in **1** (SOF = 1) and Rb2 and Rb3 in **2** (SOFs = 0.5). Cs2 and Cs3 in **3** are disordered with SOFs of respectively 0.6 and 0.4 on the basis of the least squares refinement. Related SOFs of 0.6 (for O2 and O3) and 0.4 (for O1) were determined for the water molecules of crystallization, leading thereby to the formulation of **3** as $Cs_4Sn_4Se_{10} \cdot 3.2H_2O$. The disorder in this structure leads to a relatively high wR_2 value of 0.182. Atom coordinates and equivalent isotropic temperature factors are listed for **1–3** in Table 2, bond lengths and angles are given in Tables 3 and 4. Crystallographic data for the

TABLE 2
Atom Positional Parameters with Equivalent Isotropic Temperature Factors U_{eq} (Å^2 × 10^3)[a]

Atom	x/a	y/b	z/c	U_{eq}
		$K_4Sn_4Se_{10} \cdot 4.5H_2O$ (**1**)		
K(1)	0	0	8993(4)	87(2)
K(2)	−1015(4)	1522(4)	5811(2)	83(1)
Sn(1)	0	0	6953(1)	25(1)
Sn(2)	−2734(1)	−1298(1)	7606(1)	23(1)
Se(1)	0	0	5798(1)	38(1)
Se(2)	−1288(1)	−1655(1)	7479(1)	32(1)
Se(3)	−3042(1)	−517(1)	6688(1)	40(1)
Se(4)	−2499(1)	−348(1)	8652(1)	30(1)
O(1)	−1052(16)	−1472(17)	9763(11)	66(6)[b]
O(2)	−4179(10)	546(10)	7860(7)	97(5)
		$Rb_4Sn_4Se_{10} \cdot 1.5H_2O$ (**2**)		
Rb(1)	0	0	8971(2)	69(1)
Rb(2)	−1125(3)	1438(3)	5802(2)	56(1)[b]
Rb(3)	−4091(4)	541(4)	7706(2)	91(2)[b]
Sn(1)	0	0	6967(1)	32(1)
Sn(2)	−2750(1)	−1295(1)	7612(1)	33(1)
Se(1)	0	0	5827(1)	50(1)
Se(2)	−1296(1)	−1620(1)	7491(1)	43(1)
Se(3)	−3098(2)	−564(2)	6707(1)	51(1)
Se(4)	−2535(1)	−351(1)	8643(1)	40(1)
O(1)	−1041(18)	−1538(18)	9845(9)	53(7)[b]
		$Cs_4Sn_4Se_{10} \cdot 3.2H_2O$ (**3**)		
Cs(1)	−2764(2)	−362(2)	1257(1)	51(1)
Cs(2)	7355(4)	4471(3)	3531(2)	55(1)[c]
Cs(3)	8358(5)	−4840(4)	3523(3)	51(1)[d]
Sn(1)	2479(1)	4612(1)	514(1)	21(1)
Sn(2)	1239(2)	653(1)	3491(1)	30(1)
Se(1)	293(2)	6969(2)	−271(2)	30(1)
Se(2)	5067(2)	6430(2)	780(2)	33(1)
Se(3)	2597(3)	3192(2)	2959(2)	46(1)
Se(4)	2166(4)	−944(3)	2216(2)	76(1)
Se(5)	2257(2)	−611(2)	5800(1)	38(1)
O(1)	5214(83)	−3339(70)	4518(75)	86(21)[d]
O(2)	9600(46)	−3309(37)	4081(30)	83(10)[c]
O(3)	5405(64)	−2591(40)	4062(29)	72(14)[c]

[a] U_{eq} is defined as $\frac{1}{3}$ of the trace of the orthogonalized $\mathbf{U}_{ij}$ tensor.
[b] Partial occupation factors (SOFs) of 0.5.
[c] SOFs of 0.6.
[d] SOFs of 0.4.

TABLE 3
Bond Lengths (Å) and Angles (°) in $K_4Sn_4Se_{10} \cdot 4.5H_2O$ (1) and $Rb_4Sn_4Se_{10} \cdot 1.5H_2O$ (2)

	1	**2**
Sn1–Se1	2.428(3)	2.438(3)
Sn1–Se2	2.557(2)	2.565(2)
Sn2–Se2	2.546(1)	2.562(2)
Sn2–Se3	2.438(2)	2.437(2)
Sn2–Se4	2.562(2)	2.574(2)
Se1–Sn1–Se2	115.62(4)	115.91(5)
Se2–Sn1–Se2a	102.68(5)	102.33(7)
Se2–Sn2–Se3	115.15(5)	115.78(7)
Se2–Sn2–Se4	108.76(5)	108.85(7)
Se2–Sn2–Se4c	102.60(5)	101.69(7)
Se3–Sn2–Se4	114.01(6)	114.15(8)
Se3–Sn2–Se4c	118.80(5)	118.63(8)
Se4–Sn2–Se4c	95.25(4)	95.31(6)
Sn1–Se2–Sn2	98.96(4)	100.83(7)
Sn2–Se4–Sn2c	84.75(4)	84.69(6)

TABLE 4
Bond Lengths (Å) and Angles (°) in $Cs_4Sn_4Se_{10} \cdot 3.2H_2O$ (3)

Sn1–Se1	2.547(2)	Sn1–Se1a	2.708(2)
Sn1–Se2	2.770(2)	Sn1–Se2b	2.518(2)
Sn1–Se3	2.592(2)	Sn2–Se3	2.524(2)
Sn2–Se4	2.436(2)	Sn2–Se5	2.596(2)
Sn2–Se5c	2.561(2)		
Se1–Sn1–Se1a	86.78(6)	Se1–Sn1–Se2b	128.30(7)
Se1–Sn1–Se2	88.40(6)	Se1–Sn1–Se3	119.06(8)
Se1a–Sn1–Se2b	94.88(6)	Se1a–Sn1–Se2	174.78(6)
Se1a–Sn1–Se3	95.48(7)	Se2b–Sn1–Se2	89.69(5)
Se2b–Sn1–Se3	112.21(8)	Se2–Sn1–Se3	89.09(7)
Se3–Sn2–Se4	121.78(11)	Se3–Sn2–Se5	97.74(7)
Se3–Sn2–Se5c	114.37(8)	Se4–Sn2–Se5	114.45(8)
Se4–Sn2–Se5c	112.07(10)	Se5–Sn2–Se5c	94.71(7)
Sn1–Se1–Sn1a	93.22(6)	Sn1–Se2–Sn1b	90.31(5)
Sn1–Se3–Sn2	106.92(8)	Sn2–Se5–Sn2c	85.29(7)

compounds reported in this work have been deposited at the Fachinformationszentrum Karlsruhe (D-76344 Eggenstein-Leopoldshafen, Germany) and can be obtained on citing the deposition numbers CSD 410289-410291.

RESULTS AND DISCUSSION

*Structures of $K_4Sn_4Se_{10}\cdot 4.5H_2O$ (**1**) and $Rb_4Sn_4Se_{10}\cdot 1.5H_2O$ (**2**)*

Solventothermal treatment of Sn and Se with the alkali metal carbonates K_2CO_3 and Rb_2CO_3 in a 1:2 H_2O/CH_3OH mixture at a starting pH value in the range 12–13 leads to the crystallization of the isotypic selenidostannates(IV) $K_4Sn_4Se_{10}\cdot 4.5H_2O$ (**1**) and $Rb_4Sn_4Se_{10}\cdot 1.5H_2O$ (**2**) from the respective reaction solutions. Whereas orange-red prisms of the former phase can be grown by slowly cooling the mother liquor from 130°C to room temperature, it is necessary to further cool the reaction solution to −8°C for 3 d to allow the isolation of orange crystals of **2** in a satisfactory yield. **2** can also be obtained in lower yield by simply refluxing the reaction solution prior to cooling. Careful pH control is essential for the preparation of these lamellar selenidostannates(IV). Increasing the solvent volume from 0.9 to 1.5 ml (i.e., lowering the pH value) leads to the crystallization of orange $K_6Sn_4Se_{11}\cdot 8H_2O$ (18) or black $Rb_2Sn_4Se_9\cdot H_2O$ (14) on cooling the reaction solution from 115–130°C to room temperature under similar solventothermal conditions. $Rb_6Sn_4Se_{11}\cdot xH_2O$ (18), which is isotypic with $K_6Sn_4Se_{11}\cdot 8H_2O$, may be isolated from the resulting yellow mother liquor in the latter case by allowing it to stand at −8°C for 24 h.

The asymmetric unit of the ${}^{2}_{\infty}[Sn_4Se_{10}^{4-}]$ polyanions of **1** and **2** is illustrated in Fig. 1. C_3 symmetric $SnSe_4^{4-}$ tetrahedra and C_i symmetric $[Sn_2Se_6]^{4-}$ ditetrahedra can be recognized as molecular building blocks that corner-bridge to generate the open 6^3 net of these lamellar selenidostannates(IV) (Fig. 2). The resulting 36-membered rings with their ca. 13 × 14 Å cross-sections contain four atoms more than those in $(R_4N)_2Sn_4S_9$ (7, 8) and, therefore, represent the largest known cavity size in a lamellar chalcogenidostannate(IV). Neighboring parallel sheets in **1** and **2** are stacked in the c direction at distances of respectively 7.124 and 7.006 Å so that their connecting $SnSe_4$ tetrahedra lie above the centers of the macrocyclic rings in the original anion sheet. It is also apparent, that, in contrast to $(R_4N)_2Sn_4S_9$ and other 2- or 3-dimensional thio- and selenidostannates(IV), the characteristic coordination number 4 of the solution species $SnSe_4^{4-}$ and $[Sn_2Se_6]^{4-}$ is retained in **1** and **2** after their condensation to a solid-state network.

Bond lengths and angles in the ${}^{2}_{\infty}[Sn_4Se_{10}^{4-}]$ anions (Table 3) reflect the typical trends that have been established for other chalcogenidostannates(IV) (2). The terminal more polar Sn1–Se1 and Sn2–Se3 bonds are markedly shorter (2.428–2.438 Å) than those between the tin atoms and the bridging selenium atoms Se2 and Se4 (2.546–2.574 Å). As a consequence, all Se_t–Sn–Se_b angles (t = terminal, b = bridging) are much wider (114.0–118.8°) than the ideal tetrahedral angle of 109.5°. In accordance with metrical data for other isolated $[Sn_2Se_6]^{4-}$ anions (10), the endocyclic bond angle at Sn2 (95.3°) is significantly larger than that at Se4 (84.7°).

The coordination spheres of the structure-directing rubidium cations Rb1–Rb3 of **2** are depicted in Figs. 3a–c. K1 of **1** and Rb1 occupy analogous sites on the C_3 axes of their rhombohedral crystal lattices (space group $R\bar{3}$) and exhibit a coordination number of 9 corresponding to a tricapped trigonal prism. The cations Rb2 and Rb3 are disordered (SOFs = 0.5) and display respective coordination numbers of 6 (trigonal prism) and 8 (distorted quadratic antiprism). In contrast, these general sites are fully occupied by K1 and O2 in **1**, which, as a consequence, contains 4.5 water molecules in its asymmetric unit rather than the 1.5 of the isotypic rubidium phase **2**. Two symmetry-related oxygen atoms O2 cap the faces of the Se_6 trigonal prism surrounding K2 to extend its coordination number to 8 (Fig. 3d).

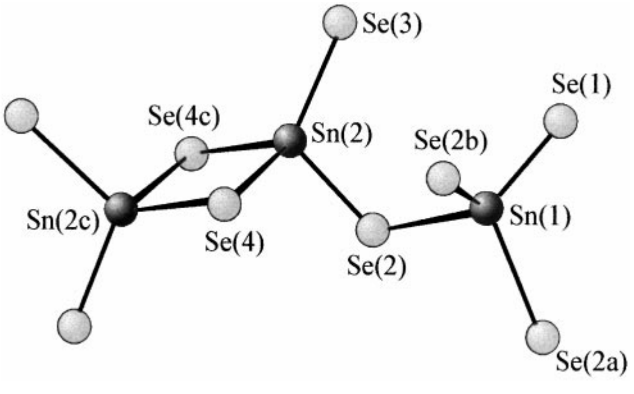

FIG. 1. Numbering scheme in the asymmetric unit of the ${}^{2}_{\infty}[Sn_4Se_{10}^{4-}]$ polyanions of **1** and **2**.

*Structure of $Cs_4Sn_4Se_{10}\cdot 3.2H_2O$ (**3**)*

The reaction of Cs_2CO_3 with Sn and Se in a 1:2 H_2O/CH_3OH mixture under similar solventothermal conditions affords a lamellar selenidostannate(IV) $Cs_4Sn_4Se_{10}\cdot 3.2H_2O$ (**3**) of the same formula type $A_4Sn_4Se_{10}\cdot xH_2O$ as **1** and **2**. However, despite its identical condensation grade of $c = 0.40$, the ${}^{2}_{\infty}[Sn_4Se_{10}^{4-}]$ anion of **3** exhibits a strikingly different structure, in which the average coordination number of the tin atoms is 4.50 as in $Cs_2Sn_4Se_9\cdot H_2O$ (14). Black crystals of this likewise lamellar selenidostannate(IV) may be obtained together with chainlike $Cs_2Sn_2Se_5\cdot H_2O$ and $Cs_2Sn_2Se_5$ (18) by increasing the solvent volume from 0.9 to 1.5 ml. In contrast, $Cs_4Sn_2Se_6$ with its discrete ditetrahedral

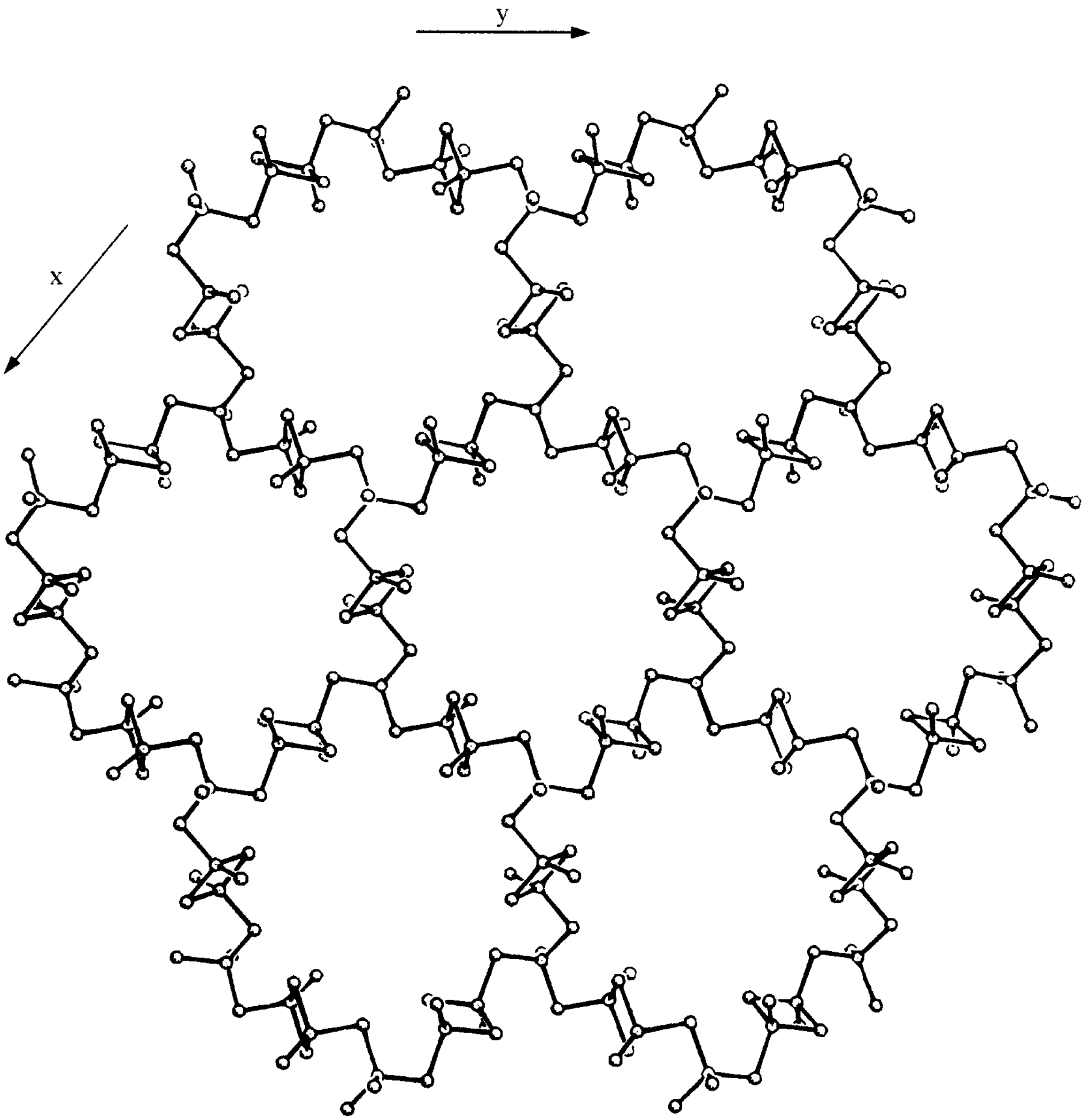

FIG. 2. The 6^3 net of the lamellar ${}^{2}_{\infty}[\mathrm{Sn_4Se_{10}^{4-}}]$ anions of **1** and **2**.

$[\mathrm{Sn_2Se_6}]^{4-}$ anions (12) can be isolated together with **3** at the higher starting pH value associated with the reduced solvent volume.

The asymmetric unit of the ${}^{2}_{\infty}[\mathrm{Sn_4Se_{10}^{4-}}]$ sheets of **3** is depicted in Fig. 4, the extended structure in Fig. 5. Parallel ${}^{1}_{\infty}[\mathrm{SnSe_3^{2-}}]$ chains with edge-bridged $\mathrm{SnSe_5}$ trigonal bipyramids can be discerned as a characteristic structural motif. These are linked by bridging $[\mathrm{Sn_2Se_6}]^{4-}$ ditetrahedra to generate the porous anion sheets of **3** with their 20-membered rings. The structure of these ${}^{2}_{\infty}[\mathrm{Sn_4Se_{10}^{4-}}]$ polyanions is closely related to that of ${}^{2}_{\infty}[\mathrm{Sn_2Se_6^{2-}}]$ in $\mathrm{Cs_2Sn_2Se_6}$ (14, 19), in which the role of the bridging $[\mathrm{Sn_2Se_6}]^{4-}$ building units is taken over by $\mathrm{Se_2^{2-}}$ dumbbells. Analogous ${}^{1}_{\infty}[\mathrm{Sn}E_3^{2-}]$ chains are also present in the framework anions of $A_2\mathrm{Sn}_2E_5$ [$E = \mathrm{S}$, $A = \mathrm{K}$ (20), Tl (21); $E = \mathrm{Se}$, $A = \mathrm{K}$ (20), Rb (15)] and $\mathrm{Na_4Sn_3S_8}$ (22). Neighboring ${}^{1}_{\infty}[\mathrm{SnE_3^{2-}}]$ ribbons are orientated at 90° to one another in these 3-dimensional chalcogenidostannates(IV) and cross-linked through respectively shared equatorial chalcogen atoms or corner-bridging $\mathrm{SnS_4^{4-}}$ tetrahedra.

The axial Sn1–Se1a and Sn1–Se2 bonds (2.708, 2.770 Å) are, as expected, markedly longer than the equatorial

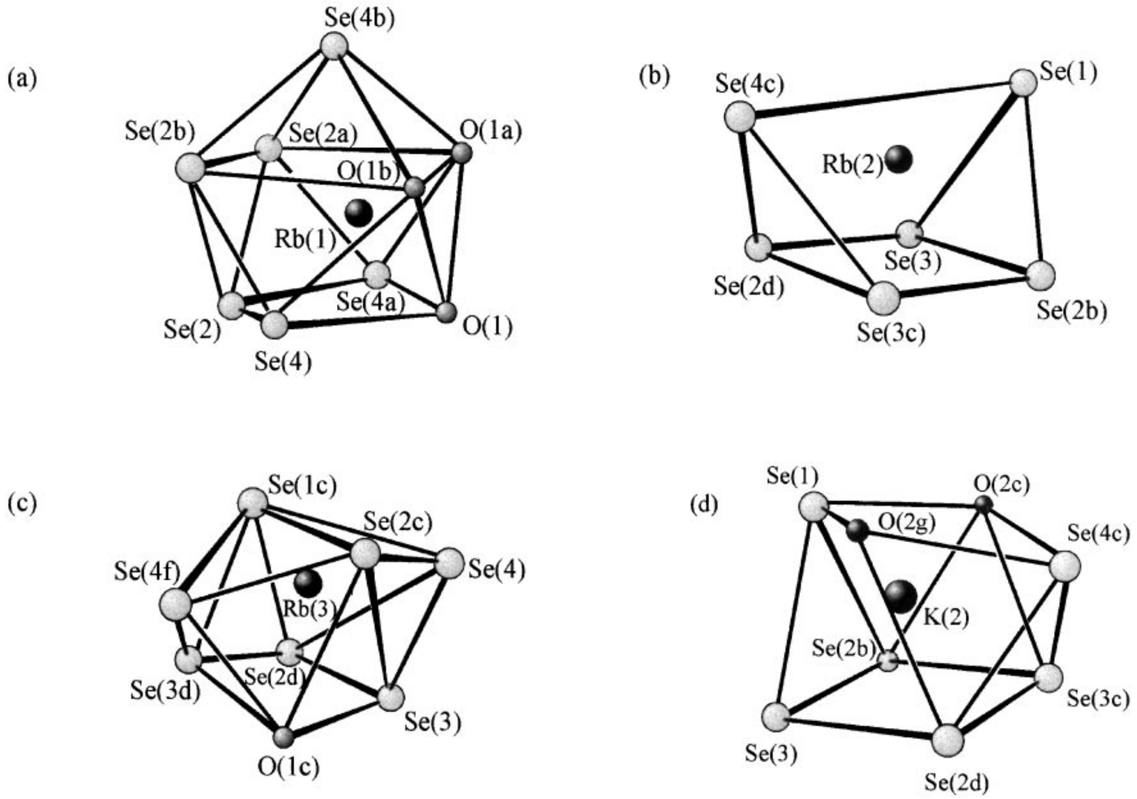

FIG. 3. Coordination spheres of the cations Rb1–Rb3 (a–c) in **2** and K2 (d) in **1**.

Sn1–Se1 and Sn1–Se2b bonds (2.547, 2.518 Å) in the $\mathrm{SnSe_5}$ trigonal bipyramids of **3**. In accordance with observations for **1** and **2**, the terminal Sn2–Se4 bonds of the $[\mathrm{Sn_2Se_6}]^{4-}$ building blocks (2.436 Å) are considerable shorter than bonds between this tin atom and bridging selenium atoms (2.524-2.596 Å). Rhombic distortion of the four-membered $(\mathrm{SnSe})_2$ rings in these ditetrahedral units may be gauged from the difference between the Sn2 ⋯ Sn2c distance of 3.494(2) Å and the accompanying Se5 ⋯ Se5c separation of 3.793(2) Å.

Coordination numbers between 7 and 9 are observed for the cesium cation of **3**, whose environments are depicted in Fig. 6. Disordering was established for the alkali metal atoms Cs2 and Cs3 and the water oxygens O1–O3 in their first coordination spheres. The cesium site Cs2 (SOF = 0.6) is occupied together with its coordination partners O2 and O3, which provide a square face of the resulting quadratic antiprismatic coordination sphere. Cs3 (SOF = 0.4) contains one of each of these oxygen sites together with O1 in its capped octahedral coordination environment. Unrealistically close contacts rule out the simultaneous occupation of potential adjacent positions of the atom pairs Cs3/O2 and O1/O3 and thereby limit the site occupation factors of the oxygen atoms to respectively 0.4 (for O1) and 0.6 (for O2 and O3) in **3**.

Solventothermal Synthesis of Selenidostannates(IV)

By employing a 1 : 2 $\mathrm{H_2O/CH_3OH}$ solution for the solventothermal reaction of $A_2\mathrm{CO_3}$ with Sn and Se, we have been successful in isolating no less than three novel lamellar selenidostannates(IV), namely ${}^{2}_{\infty}[\mathrm{Sn_4Se_9^{2-}}]$ [A = Rb, Cs (14)] and two structurally different ${}^{2}_{\infty}[\mathrm{Sn_4Se_{10}^{4-}}]$ anions [A = K, Rb; A = Cs]. As summarized in Table 5, the construction of a particular anionic network is controlled by both solution pH and alkali cation size. The role of temperature is apparent for $\mathrm{Rb_4Sn_4Se_{10} \cdot 1.5H_2O}$, which crystallizes at −8°C. A starting pH value of ca. 12 was established as a prerequisite for the required condensation of predominate solution species such as $[\mathrm{Sn_2Se_6}]^{4-}$ or $\mathrm{SnSe_4^{4-}}$ to 2-dimensional polyanions. The mother liquors exhibited pH values in the range 8–10 after isolation of the solid-state products. Ozin *et al.* have given a starting pH range of 13–14 for the preparation lamellar of alkylammonium thiostannates(IV) from $(R_4\mathrm{N})\mathrm{OH}$, Sn, and S (23). They also observed the formation of sheetlike materials at lower pH values (11–12) but were unable to fully characterize such products. O'Hare and co-workers followed the synthesis of the 6^3 nets of $(\mathrm{Me_4N})_2\mathrm{Sn_3S_7}$ under hydrothermal conditions at a starting pH between 13.7 and 14.6 using real-time *in-situ* energy-dispersive X-ray diffraction (24).

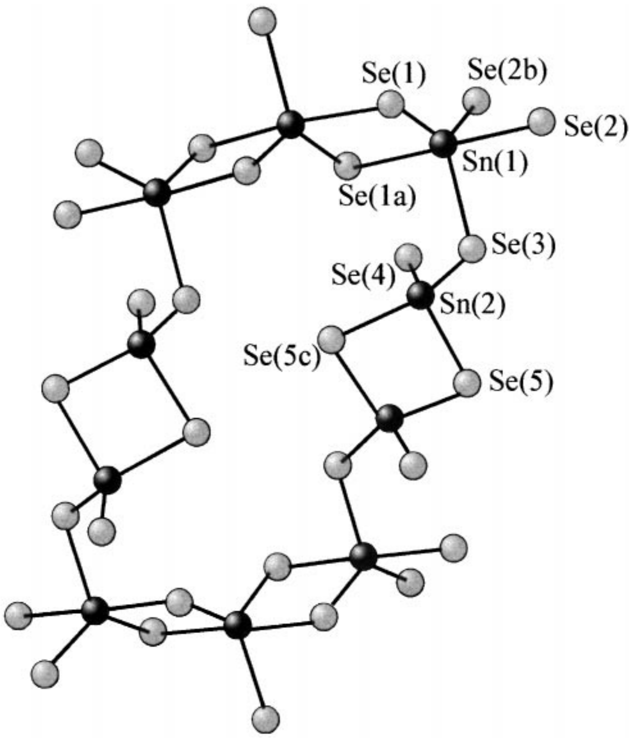

FIG. 4. Numbering scheme in the asymmetric unit of the ${}^{2}_{\infty}[\mathrm{Sn_4Se_{10}^{4-}}]$ polyanions of **3**.

It is apparent that the effective shape and size of the structure-directing aquated alkali metal cations can be readily modified by the incorporation of a variable number of water molecules in an $\mathrm{H_2O/CH_3OH}$ solventothermal reaction solution. For instance, the ${}^{2}_{\infty}[\mathrm{Sn_4Se_{10}^{4-}}]$ sheets of **1** ($A = \mathrm{K}$) and **2** ($A = \mathrm{Rb}$) are constructed in the presence of respectively 4.5 and 1.5 water molecules per formula unit. The intermediate-sized $\mathrm{Rb^+}$ cation can alternatively stabilize ${}^{2}_{\infty}[\mathrm{Sn_4Se_9^{2-}}]$ sheets, as also found for $A = \mathrm{Cs^+}$, at the lower starting pH provided by a reduced $A_2\mathrm{CO_3/H_2O}$ ratio (1.0–2.1).

In contrast to its heavier congeners, the potassium cation has only been found to direct the construction of a single sheet anion, namely ${}^{2}_{\infty}[\mathrm{Sn_4Se_{10}^{4-}}]$. However, the isolation of different phases $\mathrm{K_6Sn_4Se_{11} \cdot 8H_2O}$ (18) and $\mathrm{K_4Sn_4Se_{10} \cdot 4.5H_2O}$ (**1**) at respectively lower or higher $\mathrm{K_2CO_3/H_2O}$ ratios once again underlines the importance of pH control for such solventothermal investigations. Both the discrete $[\mathrm{Sn_4Se_{11}}]^{6-}$ anions of the former compound and the ${}^{2}_{\infty}[\mathrm{Sn_4Se_{10}^{4-}}]$ sheets of **1** contain the predominate solution species $[\mathrm{Sn_2Se_6}]^{4-}$ as a molecular building unit. The ratio of mononuclear $\mathrm{SnSe_4^{4-}}$ anions to the ditetrahedral $[\mathrm{Sn_2Se_6}]^{4-}$ species will increase as the pH rises (25) leading, thereby, to the incorporation of corner-bridged $\mathrm{SnSe_4^{4-}}$ tetrahedra as a second building block in the porous 2-dimensional anions of **1** and **2**, which can be crystallised

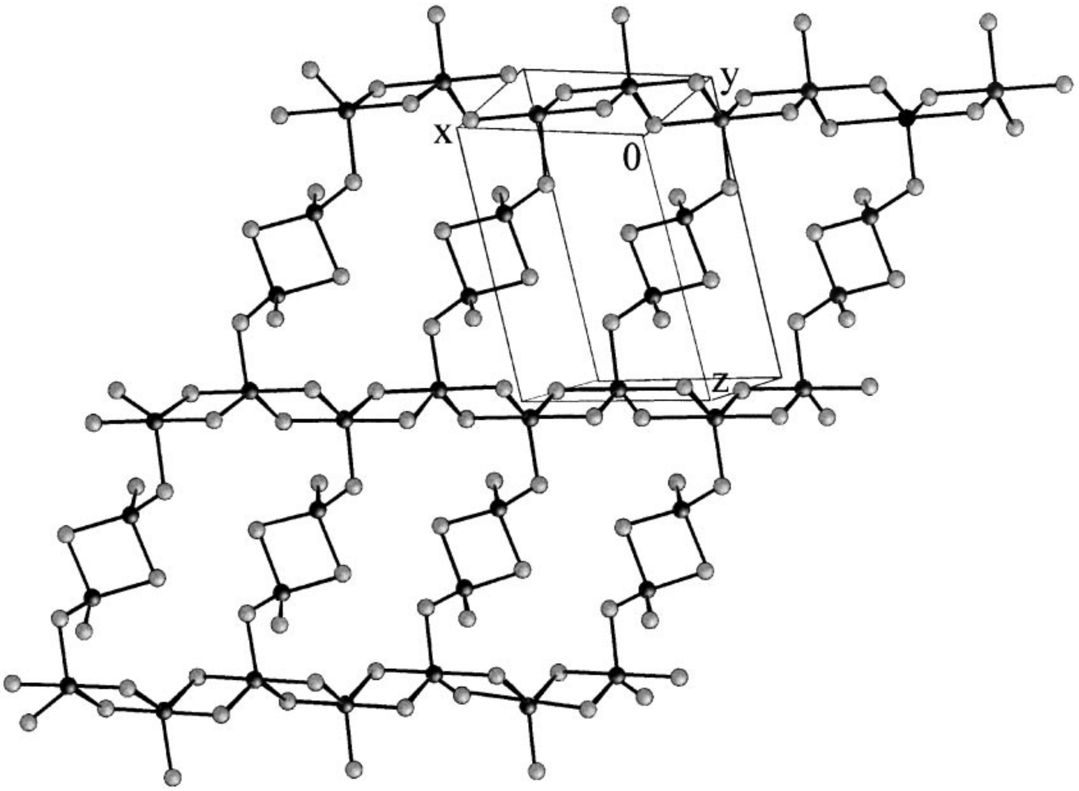

FIG. 5. The extended structure of the ${}^{2}_{\infty}[\mathrm{Sn_4Se_{10}^{4-}}]$ sheets of **3**.

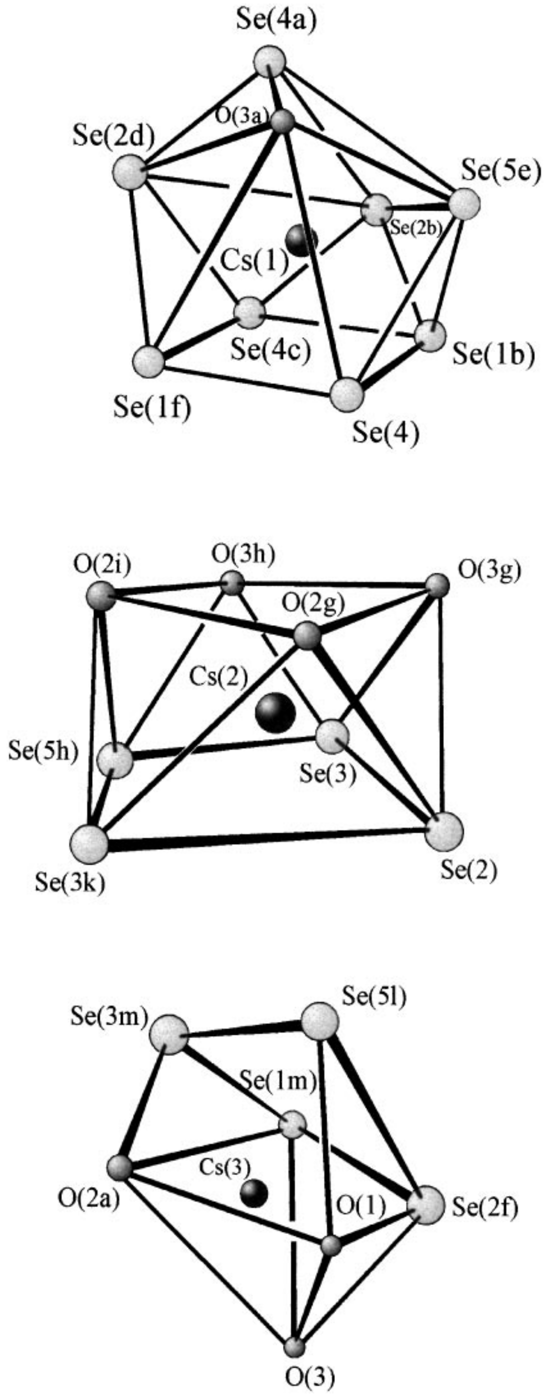

FIG. 6. The coordination spheres of the cations Cs1–Cs3 in **3**.

TABLE 5
Solventothermal Synthesis of Selenidostannates(IV) in a 1 : 2 H_2O/CH_3OH mixture at 115–130°C

Cation A	mmol (A_2CO_3)/ml (H_2O)[a]	
	1.0–2.2	3.1–3.6
K	$[Sn_4Se_{11}]^{6-}$ (18)	${}^{2}_{\infty}[Sn_4Se_{10}^{4-}]$
Rb	$[Sn_4Se_{11}]^{6-}$ (18)	${}^{2}_{\infty}[Sn_4Se_{10}^{4-}]$
Rb	${}^{2}_{\infty}[Sn_4Se_9^{2-}]$ (14)	
Cs	${}^{2}_{\infty}[Sn_4Se_9^{2-}]$ (14)	${}^{2}_{\infty}[Sn_4Se_{10}^{4-}]$
Cs	${}^{1}_{\infty}[Sn_2Se_5^{2-}]$ (18)	$[Sn_2Se_6]^{4-}$ (12)

[a] Sn:Se molar ratio = 1 : 2.

from the reaction solution at room temperature or below. As we have discussed previously (14, 18), repeated corner-bridging of $[Sn_2Se_6]^{4-}$ anions in the presence of Cs^+ cations leads to the generation of the infinite ${}^{1}_{\infty}[Sn_2Se_5^{2-}]$ ribbons in $Cs_2Sn_2Se_5 \cdot H_2O$ (18), which can subsequently link through shared previously terminal selenium atoms to construct the ${}^{2}_{\infty}[Sn_4Se_9^{2-}]$ sheets of $Cs_2Sn_4Se_9 \cdot H_2O$ (14) at a mmol (Cs_2CO_3)/ml (H_2O) ratio of 2.2. At the higher ratio of 3.1 employed in the current work, corner-sharing $[Sn_2Se_6]^{4-}$ anions take over the bridging role between parallel ${}^{1}_{\infty}[Sn_2Se_5^{2-}]$ chains to afford the ${}^{2}_{\infty}[Sn_4Se_{10}^{4-}]$ polyanions of $Cs_4Sn_4Se_{10} \cdot 3.2H_2O$ (**3**).

REFERENCES

1. R. L. Bedard, S. T. Wilson, L. D. Vail, J. M. Bennett, and E. M. Flanigen, *in* "Zeolites, Facts, Figures, Future" (P. A. Jacobs and R. A. van Santen, Eds.), p. 375. Elsevier, Amsterdam, 1989.
2. W. S. Sheldrick and M. Wachhold, *Coord. Chem. Rev.* **176,** 211 (1998).
3. W. S. Sheldrick and M. Wachhold, *Angew. Chem., Int. Ed. Engl.* **36,** 206 (1997).
4. W. S. Sheldrick, *Z. Anorg. Allg. Chem.* **565,** 23 (1988).
5. J. B. Parise, Y. Ko, J. Rijssenbeck, D. M. Nellis, K. Tan, and S. Koch, *J. Chem. Soc., Chem. Commun.* 527 (1994).
6. H. Ahari, C. L. Bowes, T. Jiang, A. Lough, G. A. Ozin, R. L. Bedard, S. Petrov, and D. Young, *Adv. Mater.* **7,** 375 (1995).
7. T. Jiang, A. J. Lough, G. A. Ozin, and D. Young, *Chem. Mater.* **7,** 245 (1995).
8. Y. Ko, C. L. Cahill, and J. B. Parise, *J. Chem. Soc., Chem. Commun.* 69 (1994).
9. W. S. Sheldrick and H. G. Braunbeck, *Z. Naturforsch., B* **45,** 23 (1990).
10. (a) W. S. Sheldrick and H. G. Braunbeck, *Z. Anorg. Allg. Chem.* **619,** 1300 (1993). (b) H. G. Braunbeck, Dissertation, University of Kaiserslautern, 1991.
11. W. S. Sheldrick and B. Schaaf, *Z. Anorg. Allg. Chem.* **620,** 1041 (1994).
12. W. S. Sheldrick and H. G. Braunbeck, *Z. Naturforsch., B* **44,** 851 (1989).
13. W. S. Sheldrick, *Z. Naturforsch., B* **43,** 249 (1988).
14. A. Loose and W. S. Sheldrick, *Z. Naturforsch., B* **53,** 349 (1998).
15. W. S. Sheldrick and H. G. Braunbeck, *Z. Naturforsch., B* **47,** 151 (1992).
16. G. M. Sheldrick, "SHELXS-86: Program for Crystal Structure Solution." Göttingen University, Göttingen, 1986.
17. G. M. Sheldrick, "SHELXL-93: Program for Crystal Structure Refinement." Göttingen University, Göttingen, 1993.
18. A. Loose and W. S. Sheldrick, *Z. Anorg. Allg. Chem.* **625,** 233 (1999).
19. K. O. Klepp and F. Fabian, *Z. Kristallogr., New Structures* **213,** 17 (1998).
20. K. O. Klepp, *Z. Naturforsch., B* **47,** 197 (1992).
21. G. Eulenberger, *Z. Naturforsch., B* **36,** 687 (1981).
22. J. C. Jumas, E. Philippot, and M. Maurin, *J. Solid State Chem.* **14,** 152 (1975).
23. T. Jiang, G. A. Ozin, and R. L. Bedard, *Adv. Mater.* **6,** 860 (1994).
24. R. J. Francis, S. J. Price, J. S. O. Evans, S. O'Brien, D. O'Hare, and S. M. Clark, *Chem. Mater.* **8,** 2102 (1996).
25. B. Krebs, *Angew. Chem., Int. Ed. Engl.* **24,** 113 (1983).